Title

Improving Groundwater Model in Regional Sedimentary Basin Using Hydraulic Gradients

Journal

KSCE Journal of Civil Engineering, 24(5)

ISSN

1226-7988

Authors

Tanachaichoksirikun, Pinit
Seeboonruang, Uma
Fogg, Graham E

Publication Date

2020-05-01

DOI

10.1007/s12205-020-1781-8

Peer reviewed

KSCE Journal of Civil Engineering (2020) 24(5):1655-1669
DOI 10.1007/s12205-020-1781-8

pISSN 1226-7988, eISSN 1976-3808
www.springer.com/12205

Water Resources and Hydrologic Engineering

Improving Groundwater Model in Regional Sedimentary Basin Using Hydraulic Gradients

Pinit Tanachaichoksirikun[a], **Uma Seeboonruang**[a], **and Graham E. Fogg**[b]

[a]*Dept. of Civil Engineering, Faculty of Engineering, King Mongkut's Institute of Technology Ladkrabang, Bangkok 10520, Thailand*
[b]*Dept. of Land, Air and Water Resources, Faculty of Hydrology, University of California, Davis, CA 95616, USA*

ARTICLE HISTORY

Received 6 October 2019
Revised 9 December 2019
Accepted 10 February 2020
Published Online 25 March 2020

KEYWORDS

Groundwater calibration
Anisotropy
Vertical hydraulic gradient
Regional sedimentary basin
Numerical modeling

ABSTRACT

Groundwater flow systems are strongly influenced by heterogeneity and anisotropy of hydraulic conductivity (K). Particularly in stratified clastic sedimentary aquifers, the vertical hydraulic gradient (dh/dz) is often very high, due to the low vertical hydraulic conductivity (K_v) or high anisotropy (K_h/K_v). However, data on the vertical hydraulic gradient to calibrate the anisotropy is seldom available. We investigated the relationship between the variable K_h/K_v and the dh/dz computed by a groundwater flow model to improve the regional parameterization using an extensive data base on 3D distribution of hydraulic head. Although it is commonly assumed that the value of K_h/K_v is 10, our values typically ranged between 10 and 10^5, because the maximum K_h/K_v was 10^5 in this regional basin. The simulations used MODFLOW-2000. We found that the high K_h/K_v contributed to high dh/dz, while identifying locations of potentially good vertical connectivity between the aquifer zones, where dh/dz is very low and difficult to measure sufficiently accurately. Sensitivity analysis of dh/dz to recharge and pumping from wells showed that recharge led to change in inflow of groundwater that led to head change, which in turn led to change in dh/dz. While, pumping contributed to aquifer outflow, as change in head drawdown around the influence zone, in turn changed dh/dz. Additionally, dh/dz in a shallower aquifer was more strongly affected by recharge and pumping.

1. Introduction

Horizontally stratified depositional environments such as fluvial, alluvial fan, and deltaic regions have considerable heterogeneity in all three spatial dimensions. These influence groundwater characteristics, especially of the hydraulic conductivity (K), its heterogeneity and vertical anisotropy (K_h/K_v) with respect to horizontal (K_h), and vertical hydraulic conductivity (K_v), which in turn affects the groundwater flow rate and pattern. Winter and Pfannkuch (1984) investigated the interaction of lake and groundwater flow under variable anisotropy in the groundwater system and found that, as anisotropy decreased, the seepage from the lake also decreased. Zlotnik et al. (2011) examined the impacts of anisotropy on groundwater system and found that the small-scale anisotropy contributed to local flow patterns, while the large-scale anisotropy affected intermediate and regional flow patterns. The clastic sedimentary systems, that form many of the world's major aquifer systems, commonly consist of alternating vertical sequences of coarse (sand and gravel) and fine (silt and clay) units, that can dramatically reduce the average or effective K_v relative to K_h (Fogg, 1986; Belitz et al., 1993; Fogg et al., 1998; Fogg et al., 2000).

Calibration of groundwater models, using groundwater fitting error and the hydraulic heads was not enough for the regional groundwater models because there was insufficient groundwater data (Du et al., 2018) and an additional technique was required. Izady et al. (2017) and Du et al. (2018) used groundwater balance technique and derived better contour matching observed and calibrated head, the key was the water balance estimation across the boundary, which gave important boundary data for further modeling. Patriarche et al. (2004), Jiménez-Madrid et al. (2017) and Štuopis et al. (2012) used the chemical concentration and

CORRESPONDENCE Pinit Tanachaichoksirikun 57601070@kmitl.ac.th Dept. of Civil Engineering, Faculty of Engineering, King Mongkut's Institute of Technology Ladkrabang, Bangkok 10520, Thailand

isotope technique, and showed the adequacy of water balance, in which the isotope dating supported the model. Hoque and Burgess (2012), Michael and Voss (2009), Sheets et al. (1998) and Sanford (2011) used the groundwater age technique and showed that their conceptual model led to improved agreement between tracer ages and simulated travel times, and also between measured and simulated heads and flows.

Data on K_v are scarce as compared to data on K_h, which can typically be measured directly through the use of well testing methods. There are also field well test methods for estimating K of aquitard layers that control the effective K_v, but the observation well data, needed for such tests is seldom available, especially for use in regional models. One can estimate effective K_v by assuming all the layers are perfectly continuous laterally, and applying the harmonic mean (Belitz et al., 1993), but the actual K of the silt and clay aquitards are seldom known, and these layers are seldom perfectly continuous laterally (Fogg et al., 2000). One way to bypass these problems is to estimate effective K_v values through model calibration by attempting to reproduce the vertical hydraulic gradients (dh/dz) measured with hydraulic head (h) data from wells of different depths. Fogg (1986) did this based on regional mapping of dh/dz values that showed general trends in dh/dz can indeed be used to demonstrate that the commonly small ratios between horizontal and vertical hydraulic gradients (e.g., on the order of 10^2) cannot be reproduced without quite large ratios in K_h/K_v (e.g., on the order of 10^4). Fogg (1986) also found that the computed dh/dz in the model are very sensitive to K_v. For example, he found that where zones of enhanced vertical connectivity exist, vertical groundwater fluxes can become extremely high locally, with the dh/dz values becoming quite low. In other words, when one has dh/dz data, it can not only be invaluable for calibrating K_h/K_v, but it can also indicate where zones of good local vertical connectivity might exist. Identifying such zones can be very important for modeling multi-aquifer dynamics, mapping recharge areas for deep aquifers, and identifying vulnerability of deep aquifers to contamination. Samper-Calvete and García-Vera (1998) compared isotropic and anisotropic groundwater models in Los Monegros, Northeastern Spain and found that anisotropy played a major role in the lower aquifer and led to a better match to measured heads and a more realistic representation of the hydrogeological conditions. Heilweil and Hsieh (2006) determined anisotropy in Navajo Sandstone, Southwestern Utah, using the minimum of three observation wells method, and revealed that the transmissivity in each direction could be used to derive approximate anisotropy values, from which local discontinuities could be inferred. Michael and Voss (2009) estimated regional scale groundwater properties (K and K_h/K_v), using hydraulic heads, ^{14}C concentrations and driller logs and found that a high value of vertical anisotropy indicated disconnected aquitards, which, if numerous, could strongly control the equivalent hydraulic parameters of the aquifer system.

To calibrate K_v, following Fogg (1986), however, one needs data on not only lateral hydraulic gradients, but also the vertical gradients. Such 3D h mapping is still much less common than the more typical, 2D h mapping, and cases having fully 3D h characterization over a region are rare. In this study of the Lower Chao Phraya (LCP) Basin, Thailand, there exists an unusually comprehensive 3D mapping of h. This allows us to perform an unusually detailed exploration of the interplay between model anisotropy and computed vertical and lateral hydraulic gradients. Moreover, the 3D data and model allow us to explore the possibility of using the dh/dz data to ascertain possible locations of good vertical connectivity.

Thailand's Lower Chao Phraya (LCP) basin (100°33'1" E, 14°21'19" N) was selected for investigation for three reasons: 1) it is the largest groundwater aquifer in Thailand and covers Bangkok, the capital city, 2) intensive groundwater pumping has led to water resource sustainability concerns, for example groundwater overdraft and land subsidence, and 3) it has extensive three-dimensional hydraulic head data, that presents an opportunity to identify the values of vertical hydraulic gradients and to calibrate the upscaled anisotropy.

We investigated the inverse three-dimensional groundwater flow model in the LCP basin to determined anisotropy, using the hydraulic gradient technique, because it is very sensitive to K_v values (Fogg, 1986). First, we describe the study area, including location, hydrogeology and groundwater problems. Then, we discuss the main data, from groundwater monitoring and measured hydraulic gradient, from which the groundwater model was constructed. Then details of the calibration for variable anisotropy, e.g. hydraulic head and gradient matching, are provided. Since the hydraulic gradient is also sensitive to the groundwater recharge and pumping, sensitivity analysis is included.

2. Study Area

2.1 Location and Groundwater Development

Figure 1(a) shows Thailand's LCP basin, located in the central plain, which covers 21 provinces including Bangkok (capital city). In this triangular basin, the northern tip is in Kamphaeng Phet province, and the base covers Chao Phraya River delta along the shore of the Gulf of Thailand. The plain is ~220 km from east to west and ~300 km from north to south, with a total area of 43,300 km^2. The western part of LCP basin bounds the Tenasserim hills. The northern part is the Upper Chao Phraya basin which Chao Phraya River flows and the eastern part is bounded by a series of small hills. The southern part connects to the Gulf of Thailand. It has four major rivers, the Chao Phraya, Mae Klong, Pa Sak and Tha Chin Rivers. Bangkok clay is found from the Gulf of Thailand to Ayutthaya province. The basin is relatively flat with water flowing from the north to south. The highest point is ~60 m above mean sea level (MSL) and the lowest altitude at sea level: the average elevation is 15 m above MSL Fig. 1(b).

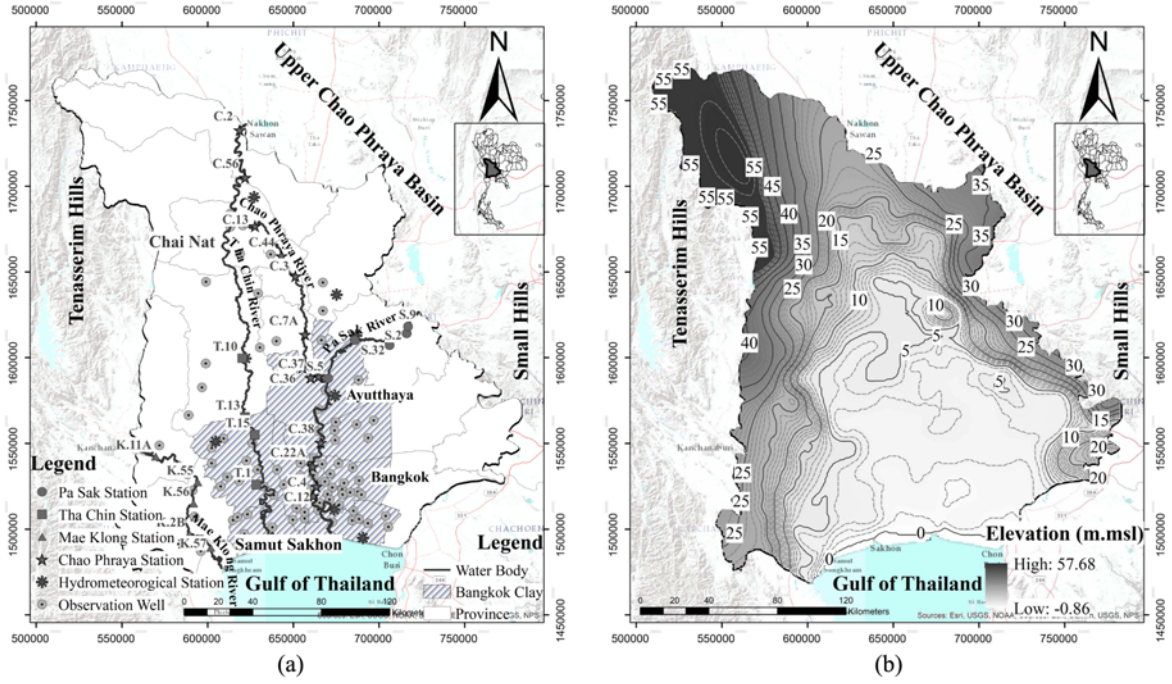

Fig. 1. Thailand's Lower Chao Phraya Basin: (a) Location Map, (b) Elevation Map

2.2 Geology

2.2.1 Geologic Framework Related to Groundwater

The Thai Department of Mineral Resource (2001) and the Thai Department of Groundwater Resources (DGR) (2015) showed the geologic formations could be classified into three age ranges. The LCP basin consists of unconsolidated and semi-consolidated sediments aged from the Tertiary-Quaternary, including coastal deposits (Q_m), e.g., the beach, mangrove, swamp, marsh, and fluvial deposits (Q_f), e.g., flood plains, alluvium, terrace and colluvium. Piancharoen (1977) and Piancharoen and Chuamthaisong (1978) concluded that, during these periods, the depositions probably occurred under fluvial and deltaic environments, with occasional shallow sea sedimentation. During the Permian, deposits belonged to the Ratchaburi (P_r) and Saraburi (P_s) Groups. The P_r group consisted of dry and hard clays, including limestone, dolomitic limestone, chert, dolomite and granite. The P_s group was composed of hard clays, including limestone, chert, basalt, ultramafic and serpentinite. The P_r and P_s groups were the uplands at the southwest (P_r) and southeastern (P_s) portions of the basin. The P_r and P_s groups are relatively low in *K*. In the rainy season, water may be lacking, because the clays hinder the recharge. In the Devonian, the Thong Pha Phum Group (SDC), e.g., calcareous shale, shale, chert, siltstone and limestone deposits, formed the upland at the western side. The permeability was low in *K*, due to the dense clay lenses. Then, soil groups were classified as impermeable rock, due to the low *K*.

The aquifer system consists mainly of Pliocene–Pleistocene–Holocene fluvial and deltaic sands, gravels and fine-grained deposits (silts and clays). These sediments compose eight principal confined aquifers with thicknesses of 30 – 70 m, each including the Bangkok (BK), Phra Pradeang (PD), Nakorn Luang (NL), Nonthaburi (NB), Sam Khok (SK), Phayathai (PT), Thonburi (TB), and Pak Nam (PN) aquifers as described by Seeboonruang (2014) and Seeboonruang (2018). The maximum thickness of the basin near the Gulf of Thailand is ~2,000 m, but it was studied to only ~600 m depth. The top of the BK aquifer from the Gulf of Thailand to Ayutthaya has Bangkok clay (BKC), soft

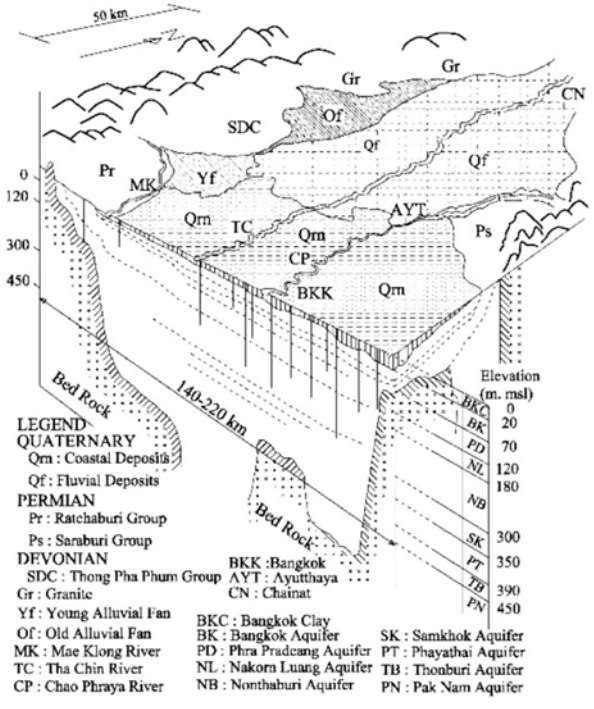

Fig. 2. Stratigraphy of LCP Basin (Adapted from Phien-wej et al., 2006)

clay with a depth 0 – 20 m below ground surface. In addition, all aquifers have clay lenses, on the top and bottom of each one, and are confined aquifers, as shown in Fig. 2.

2.2.2 Aquifer-Aquitard Stratigraphy

Sediments in Thailand's LCP basin were deposited mainly by fluvial-deltaic processes. The part of the basin underlying the Gulf of Thailand consists mostly of Quaternary marine clay from 130 – 140 m to 350 – 400 m depth. During this period, sea level rise and fall due to the ice ages resulted in fine-grained marine deposits that extended from the present-day shoreline to the middle of LCP basin and as far north as Chai Nat. The most recent marine transgression was 6,500 years ago (DGR, 2010). Later, in the Holocene, aggradation of the terrestrial fluvial-deltaic systems deposited the shallowest parts of the aquifer system. In the Pleistocene, most of sediments consisted of various sizes of gravel, sand, silt and clay, that was deposited in layers and lenses. The sediment was borne by rivers and streams and its deposition depended on the slope of the area: sediments from the Pleistocene have been penetrated by groundwater wells at depths of about 30 – 600 m.

2.2.3 Fraction of Sediments

DGR (2015) studied four of the groundwater aquifers (BK, PD, NL, NB): lithology was analyzed using 4,492 bore logs, including electrical resistivity logs and core samples, and concluded that the LCP basin consisted of 39.2% fine, 54.2% sand, 5.6% gravel and 1.0% of other types. The bore logs were collected along eight LCP tracks - four along an east-west axis and the others along a north-south axis. The fraction of sediment in each aquifer is shown in Table 1. The stratified sedimentary nature of these coarse and fine units give rise to the high values of K_h/K_v ratio.

2.3 Groundwater Resource Problems

2.3.1 Overdraft

Thailand's LCP basin is the largest groundwater basin with a yield ~100 – 300 m^3/hr (Japan International Cooperation Agency, JICA, 1995). Most of rainfall recharge to groundwater in the north and west of the region is enhanced by land use and soil permeability. Groundwater development for the public water supply, began in 1954, with an extraction of 8,360 m^3/day (Gupta and Babel, 2005). The daily groundwater extraction continuously increased over the years and more private wells were commissioned in some areas, because groundwater was free and public water supply was not available. The LCP basin had a groundwater overdraft, because total pumping exceeded 1.4 million m^3/day by 1982. Groundwater levels dropped and contributed to land subsidence and seawater intrusion. After 1983, DGR (2012) attempted to reduce groundwater extracted, by charging for water pumped, whereas tap water was supplied at a lower fee. The pumping rate decreased from 1985 – 1990. However, overdraft groundwater pumping started again in 1991 and DGR continued to charge a higher fee to control the ground-water level. By early 1997, the total groundwater withdrawal in four provinces (Bangkok, Samut Prakarn, Nonthaburi and Pathum Thani) was 1.67 million m^3/day (Ramnarong, 1999). Groundwater well data indicated that the total withdrawal by private wells was over 2 million m^3/day from 1998 – 2001. By 2003, the pumping rate decreased to 1.7 million m^3/day (Kasetsart University, 2004). From then to now, although, there were more than 19,000 groundwater pumping wells, pumping decreased to ~0.65 million m^3/day. The groundwater levels in the City of Bangkok correspondingly increased, because most people used the tap water and reduced groundwater pumping, and have been close to the ground surface in recent years. The hydraulic heads increased at rates of up to 2 m/year in some areas. However, the lowest observed hydraulic head was 60 – 70 m below MSL in the NL and NB aquifers at Samut Sakhon province in 2009 and 2014 (Fig. 3), indicating ongoing groundwater overdraft.

The groundwater overdraft contributed to the land subsidence that affected groundwater properties, as described in section 2.3.2.

Table 1. Materials in the LCP Basin

Aquifer layer	Material (%)			
	Fine (Silt/Clay)	Sand	Gravel	Other
BK aquifer	36.4	61.1	2.1	0.4
PD aquifer	44.1	50.9	4.2	0.8
NL aquifer	39.3	45.1	14.0	1.6
NB aquifer	37.1	59.7	2.1	1.1
Average	39.2	54.2	5.6	1.0

2.3.2 Land Subsidence

Cox (1968) reported subsidence from groundwater overdraft in Southeast Asia. From 1978 to 1981, the Royal Thai Survey Department (RTSD) created benchmarks for surface elevations. From then, the Asian Institute of Technology, AIT (1981) measured subsidence in the LCP area. The maximum observed subsidence was 540 mm: the maximum rate was 100 mm/year. Moreover, the average ground settlement was 114 mm. Although control of groundwater pumping started in 1983, the subsidence rate, in the suburb areas (Samut Prakarn, east Bangkok and Samut Sakhon), still increased to 30 – 35 mm/year, due to response time delay to settling. However, recently, RTSD surveyed land subsidence based on 67 benchmarks: they reported that most of benchmarks showed that the rate of subsidence in Bangkok and its vicinity, decreased slightly: the annual subsidence became 10 – 30 mm. This showed that the ground settlement rate reduced, because of groundwater control, as shown in Table 2.

Land subsidence affected the groundwater recharge, because land subsidence contributed the consolidation of clay, that, in turn, led to decrease in hydraulic conductivity (Galloway and Burbey, 2011). Additionally, it impacted groundwater pumping, because the land subsidence allowed seawater intrusion, when groundwater was pumped, and groundwater hydraulic head was

Table 2. Significant Hydraulic Events Effecting the LCP Basin

Timeline	Pumping	Hydraulic head	Land subsidence	Hydraulic gradient	Comment
prior to 1982	↑	↓	n/a	n/a	First time to observe subsidence
1983 – 1990	↓	↑	↑	n/a	DGR started to control the groundwater level
1991 – 1997	↑	↓	↑	n/a	Groundwater over pumped again
1998 – 2003	≈	≈	≈	≈	Maximum groundwater withdraws
2003 – 2009	↓	↑	≈	↑	Maximum observed subsidence
2009 – 2014	↓	↑	↓	↑	Samut Sakhon's hydraulic head in NL and NB aquifers were still low
2014 – now	≈	↑	↓	≈	Benchmarks slightly decreased the rate of subsidence in Bangkok and its vicinity

Note: ↑ = increase, ↓ = decrease, ≈ = constant, n/a = no data available

decreased 40 times compared to the seawater head, expressed by the Ghyben and Herzberg equation (Sun et al., 1999; Galloway and Burbey, 2011).

3. Data and Methods

We used the finite-difference groundwater flow model of the U.S. Geological Survey (Harbaugh et al., 2000). The governing equations for three-dimensional saturated flow combined Darcy's Law and the principle of conservation of mass (Bear, 1972). The general form of the equation for groundwater flow over the physical dimension is:

$$\frac{\partial}{\partial x}\left[K_h\frac{\partial h}{\partial x}\right]+\frac{\partial}{\partial y}\left[K_h\frac{\partial h}{\partial y}\right]+\frac{\partial}{\partial z}\left[K_v\frac{\partial h}{\partial z}\right]+W_s=S_s\frac{\partial h}{\partial t} \quad (1)$$

where K_h and K_v are the horizontal and vertical hydraulic conductivity, (dimensions LT^{-1}), h is the hydraulic head (dimension L), S_s is specific storage (dimension L^{-1}), W_s is sink or source (dimension T^{-1}) that showed external flow stresses such as pumping, recharge, and rivers. The hydraulic gradients, $\partial h/\partial x$, $\partial h/\partial y$ and $\partial h/\partial z$, are replaced by dh/dx, dh/dy and dh/dz (dimensionless), in the following, and the anisotropy is K_h/K_v (dimensionless).

3.1 Groundwater Monitoring

Although the LCP basin had more than 650 monitoring stations in 2014, only 273 stations were selected in this study, because we had comprehensive data from 2009 to 2014 for them, distributed over the PD, NL and NB aquifers as showed in Fig. 1(a).

The available observation wells, distributed across the whole basin, were installed by considering contamination, flow direction and geologic structure. Each station consists three observation wells screened separately in three aquifers (PD, NL and NB). The screen height depended on the aquifer level: the screens were only one meter high to minimize disturbance of the groundwater level. DGR observed the groundwater level in the well using a portable sounder, piezometer and electric tape measure, so the ground surface was the datum. Moreover, to reduce the tape measure error from bow, a small PVC pipe was installed for guiding the tape. Then, groundwater levels were corrected to the elevation from MSL.

A contour map, interpolated, using the inverse distance method and DGR data for hydraulic heads from 273 wells, in 2009 and 2014 is shown in Fig. 3 (DGR, 2015). We can observe that the hydraulic heads in 2009, for the PD, NL and NB aquifers, are alarmingly low, with levels as low as -25 m in PD, -45 m in NL and -60 m in NB, largely due to the excessive groundwater extraction for industrial use. Although most of the land in the study area is agricultural, the hydraulic head beneath croplands is not deep, because groundwater pumping wells, supporting agricultural irrigation, are widely spaced, and much of the water supply is provided by surface water. Toward the Gulf of Thailand, however, where industrial and urban water demands are high, groundwater extraction rates are quite high, especially in the NB aquifer. As shown in Fig. 3, between 2009 and 2014, the head increased noticeably because of higher pumping rates, despite fewer wells.

3.2 Measured Vertical Hydraulic Gradients

Data on dh/dz to calibrate K_h/K_v are seldom available, because the common groundwater model focused only on the hydraulic head. Here, dh/dz values were computed for the PD-NL and NL-NB aquifer pairs for 2009 and 2014 as shown in Fig. 4. We averaged h over 1 × 1 km^2 grid cells, differences in h values from pairs of adjacent grid cells were divided by the difference in mid-point elevations of the aquifers. In monitoring stations, the wells were sufficiently close in well nests that we determined dh/dz directly. The screens were only a meter high, so no well was in more than one aquifer. Then, h data was used for calculating dh/dz.

Positive vertical hydraulic gradients indicated upper–to–lower groundwater flow: most measured gradients were positive, thus, regionally, vertical groundwater flow was mostly downward, driven by recharge from rainfall and groundwater pumping from wells. However, some zones had negative gradients, i.e., flow was reversed or lower–to–upper in the aquifers, due either to groundwater discharge to the surface or locally greater rates of pumping in the upper aquifers. Zones of upward flow were more prevalent in the deeper NL-NB (Figs. 4(c) and 4(d)) zone than in PD-NL (Figs. 4(a) and 4(b)).

In general, the vertical hydraulic gradients were strongly downward along the northern, eastern and western boundaries of the basin and decreased to lower values, toward the interior and

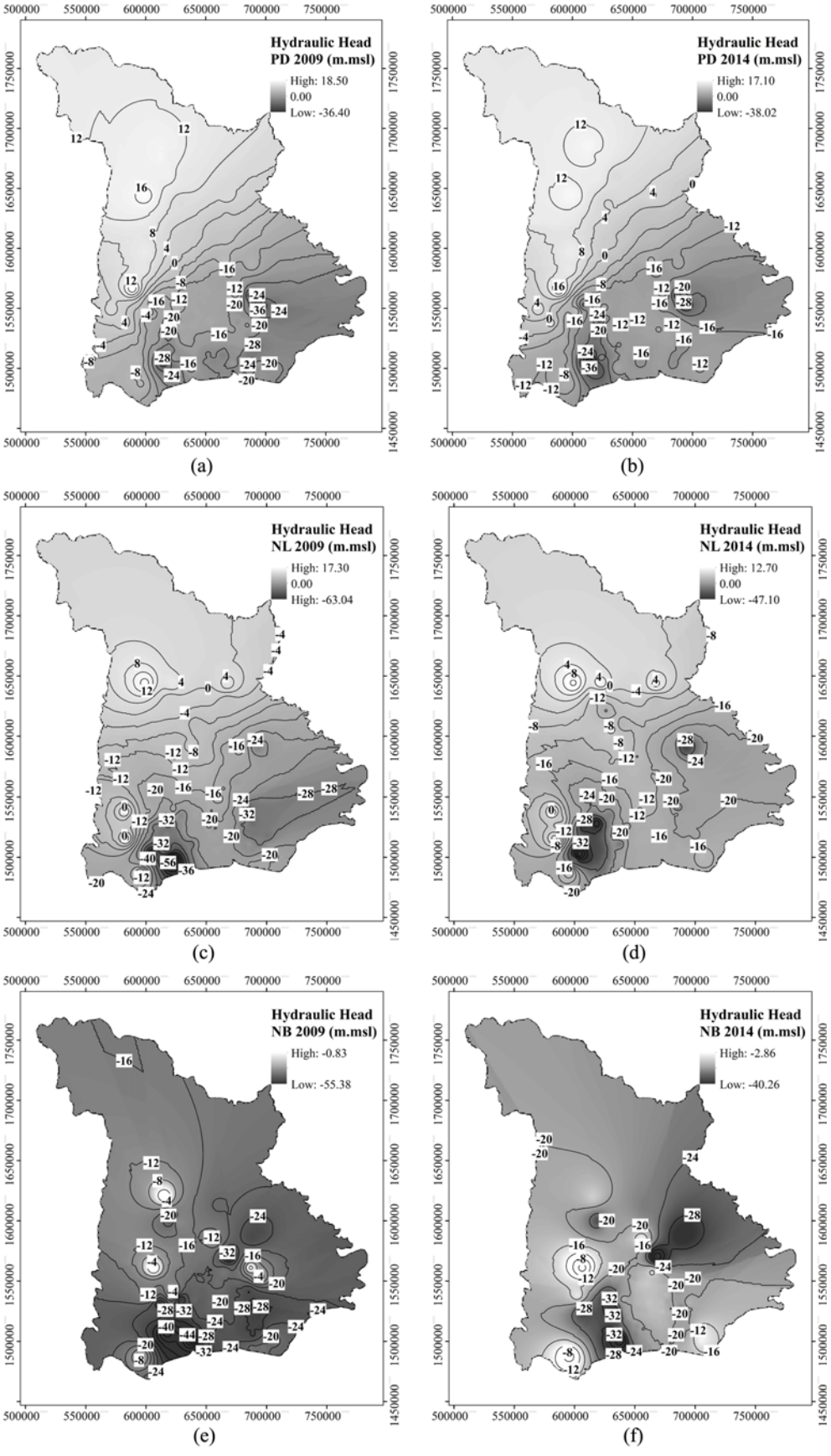

Fig. 3. Hydraulic Head: (a) PD in 2009, (b) PD in 2014, (c) NL in 2009, (d) NL in 2014, (e) NB in 2009, (f) NB in 2014

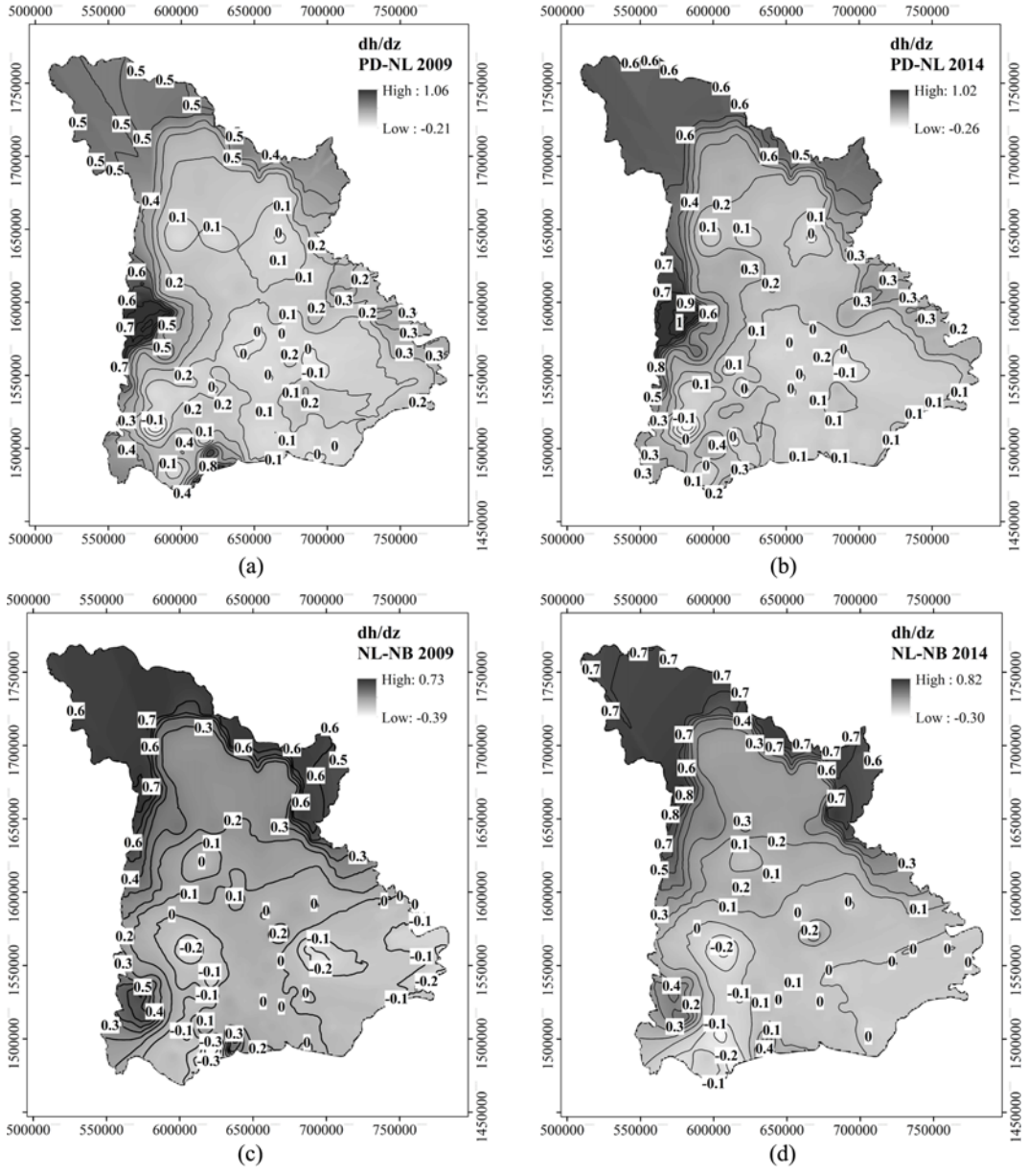

Fig. 4. Vertical Hydraulic Gradients Based on Measured Data: (a) PD-NL in 2009, (b) PD-NL in 2014, (c) NL-NB in 2009, (d) NL-NB in 2014

the coast. dh/dz magnitudes varied mainly due to pumping, recharge and K_v. The high dh/dz in the uplands were likely due to higher rates of recharge in those areas. The higher rate of recharge contributed the higher h in the upper aquifer but, in the lower aquifer, h remained constant. The differential h led to increased dh/dz. In some areas, $dh/dz \approx 0$ indicated good vertical interconnection due to local high K_v (Fogg, 1986).

$dh/dz \approx 0$, surrounded by higher dh/dz values, indicated local zones of interconnection where $K_v \approx K_h$. In that case, dh/dz values can drop to be the same order as dh/dx, which, in this basin, is ~10^{-3}. In that case, accurate dh/dz could not easily be determined, because small errors in h and small vertical distances between the well screens can obscure the exact dh/dz values. In the dh/dz map, such zones show up as effectively $dh/dz \approx 0$. Somewhat counterintuitively, such zones of low dh/dz can support the highest vertical flow rates. In contrast, we were able to measure very low dh/dx values, despite errors in h because the wells are km apart.

3.3 Groundwater Modeling of the Lower Chao Phraya Basin

MODFLOW-2000 was developed by Harbaugh et al. (2000) at the U.S. Geological Survey; it was used for LCP basin groundwater modeling, because it is a three-dimensional finite difference model, capable of simulating flows in an aquifer system, as well as handling saturated flow with homogeneous, heterogeneous, isotropic, and anisotropic aquifer systems, under steady state and transient conditions (Dawoud and Allam, 2004). This model

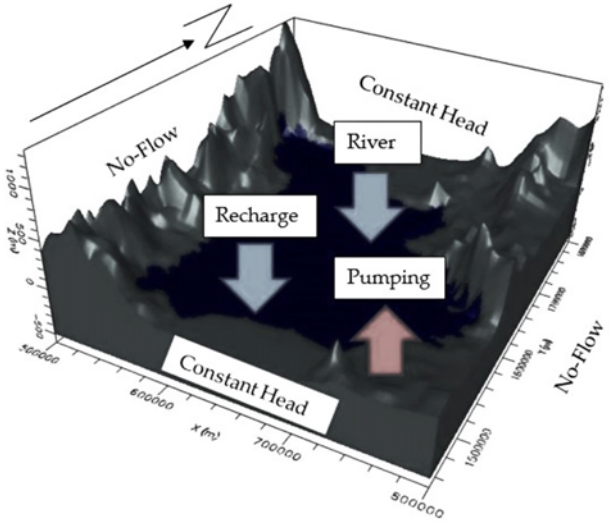

Fig. 5. 3D Groundwater Model of the LCP Basin (Tanachaichoksirikun et al., 2018)

used physiography, geology, hydrogeology, rainfall patterns, constituent rivers and groundwater extraction data from 2009 to 2014 (Arlai and Koch, 2006; DGR, 2012; Fornés and Pirarai, 2014; Taweesin et al., 2018).

Figure 5 depicts the LCP basin conceptual model and boundary conditions and its eight aquifers. The conceptual model was divided into nine layers, consisting of the eight aquifers and a top layer of Bangkok clay (BKC). The nine layers were divided into 1 km^2 cells - 350 rows × 300 columns - a total of 945,000 cells. The aquifer parameters and boundary conditions were described in section 3.4 – 3.6. An anisotropy of 10 was chosen for the first calculation, because this is a common assumption of groundwater modelers, such as DGR (2010), Saraphirom et al. (2013), Taweesin et al. (2018).

3.4 Aquifer Parameters

Characterization of the aquifer parameters was derived from DGR (2012). The hydraulic conductivity is usually the important parameter for groundwater models. The K_h is derived from averages calculated from pumping tests. Here, the K_h was characterized by underlying aquifer-aquitard stratigraphy and the faction of sediment as well, as shown in Table 3. The hydraulic conductivity of BKC was estimated to be $1 \times 10^{-8} – 1 \times 10^{-9}$ m/s, following JICA (1995).

JICA (1995) suggested setting the specific storage (S_s) in confined aquifers as $1 \times 10^{-6} – 1 \times 10^{-4}$ based on Todd and Mays (1980). S_s was not determined because its uncertainty is much

Table 3. Parameters for Groundwater Model Layers (DGR, 2012)

Aquifer layer	K_h (m/s)	Specific yield (S_y)	Specific storage (S_s, m^{-1})
BKC and Unconfined	$1 \times 10^{-5} – 1 \times 10^{-9}$	0.03 – 0.35	–
BK	$5 \times 10^{-5} – 5 \times 10^{-6}$	–	$1.10 \times 10^{-5} – 4.80 \times 10^{-5}$
PD	$2 \times 10^{-5} – 7 \times 10^{-6}$	–	$3.35 \times 10^{-5} – 4.50 \times 10^{-6}$
NL	$1 \times 10^{-4} – 6 \times 10^{-6}$	–	$3.85 \times 10^{-5} – 9.50 \times 10^{-6}$
NB	$2 \times 10^{-4} – 7 \times 10^{-6}$	–	$3.95 \times 10^{-5} – 9.50 \times 10^{-6}$
SK	$1 \times 10^{-4} – 6 \times 10^{-6}$	–	$1.00 \times 10^{-4} – 1.15 \times 10^{-5}$
PT	$1 \times 10^{-4} – 5 \times 10^{-6}$	–	$1.35 \times 10^{-5} – 3.85 \times 10^{-5}$
TB	$1 \times 10^{-4} – 6 \times 10^{-6}$	–	$1.15 \times 10^{-5} – 2.60 \times 10^{-5}$
PN	$5 \times 10^{-5} – 7 \times 10^{-5}$	–	$1.65 \times 10^{-5} – 5.00 \times 10^{-6}$

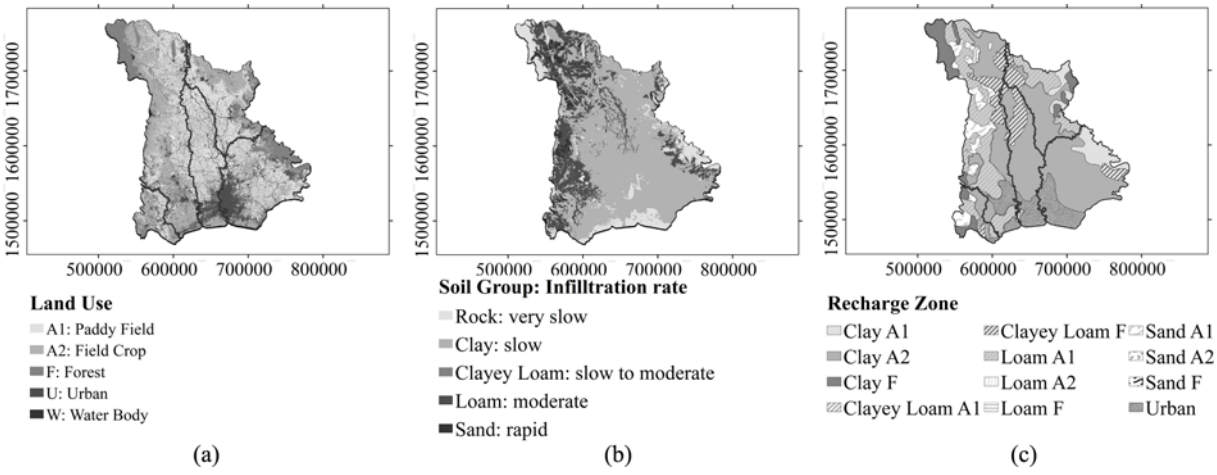

Fig. 6. Land Use, Soil Group and Recharge Zone. Recharge Zone Estimates Based on the Thai Land Development Department (LDD) (2015) Data: (a) Land Use, (b) Soil Group, (c) Recharge Zone

lower than the others i.e., K_s, pumping and recharge.

3.5 Recharge Boundary Condition

The Thai Land Development Department (LDD) (2015) divided land use in the LCP basin into five categories: 40% for *A2*: paddy field, 22% for *A1*: field crop, 15% for *F*: forests, 15% for *U*: urban and 8% for *W*: water body (i.e., rivers) - see Fig. 6(a). In addition, soil group was assigned to five categories: clay 72% of the total area; loam 16%; clayey loam 6%; sand 4% and rock 2% - see Fig. 6(b).

Furthermore, the rainfall pattern in the LCP basin is influenced by the Northeast Asian monsoon from China, that is responsible for a dry and cool season between November and February; and the Southwest Asian monsoon, that brings rain from the Gulf of Thailand, between June and September. According to the Thai Meteorological Department (TMD) station in Fig. 1(a), 10 hydrometeorological stations are available (TMD, 2015). The annual rainfall in the LCP basin, between 2009 and 2014, varied from 1,300 to 2,000 mm. Specifically, Pathum Thani province had the highest monthly rainfalls (535 mm) in September 2010, while the capital Bangkok had the highest average monthly rainfall (142 mm), particularly in the areas close to the Gulf of Thailand. In addition, the rainy season (June–September) accounts for 60% of the annual rainfall in the LCP basin.

We overlayed the land use (Fig. 6(a)) and soil group (Fig. 6(b)) to the recharge zones, based Saraphirom et al. (2013) and Pholkern et al. (2018) technique, as shown in Fig. 6(c). Note that the water body was assigned in river boundary. The Clay *A2* area is the largest recharge zone (43%), whereas the smallest is Sand *F* (0.05%).

The Thiessen polygon method divided the area of influence of rainfall in each hydrometeorological station. Then, the recharge rate boundary was generated by overlaying the recharge zone and the Thiessen polygon area. Then, the hydraulic conductivity and recharge rate values were adjusted by changing these parameters, based on the transient state simulation, so that the simulated and actual hydraulic heads were comparable. Although, the recharge rate and hydraulic conductivity were adjusted at the same time, the recharge values were adjusted in the range reported by DGR (2012). The recharge rate in the LCP Basin was adjusted to a range of 8 – 12% of rainfall (DGR, 2012). In addition, the recharge rate for Bangkok and vicinity, that was considered urban in the land use map, was estimated as ~1% of rainfall, because the city surface was mostly paved with concrete. So, the measured and simulated hydraulic heads were matched. The water body (i.e., rivers) was not considered as a recharge boundary, because it was assigned in the river boundary, so the recharge rate was set to 0% of rainfall.

3.6 Other Boundary Conditions

3.6.1 No-Flow Boundary Condition

The LCP basin is connected to the Tenasserim mountain range in the west: it was assumed to divide the groundwater, so the western edge was treated as a no-flow boundary. Similarly, the small hills to the east were treated as no-flow boundary.

3.6.2 Constant Head boundary Condition

The northern edge is separated the LCP basin with the Upper Chao Phraya basin, so was considered a constant head boundary, using measured hydraulic heads near the north edge. Similarly, the southern part of LCP basin connects to the Gulf of Thailand, so that groundwater and seawater are interconnected. Thus, the Gulf of Thailand was treated as a constant head boundary: the heads in wells near the shore were adjusted to MSL.

3.6.3 Rivers Boundary Condition

The LCP basin has four main rivers: the Chao Phraya, Mae Klong, Pa Sak, and Tha Chin Rivers. Fig. 1(a) illustrates the runoff monitoring stations, whose data was used in the river boundary, where C_i denotes the stations along the Chao Phraya (13 stations), K_i stations on the Mae Klong (5 stations), S_i on the Pa Sak (5 stations), and T_i on the Tha Chin (4 stations) rivers. The riverbed conductance, *COND*, in dimension L^2T^{-1}, was calculated, following Harbaugh et al. (2000):

$$COND = \frac{RCHLNG \times RBWIDTH \times K_z}{RBTHICK} \tag{2}$$

where *RCHLNG* is the reach length of the river in each grid cell (dimension L), *RBWIDTH* is the riverbed width in each grid cell (dimension L), *RBTHICK* is the riverbed thickness in each grid cell (dimension L), and K_z is the riverbed vertical hydraulic conductivity (dimension LT^{-1}).

River boundaries were calculated using river package in MODFLOW-2000 (Harbaugh et al., 2000). The reach length (*RCHLNG*) was digitized from the river line. The riverbed width (*RBWIDTH*), riverbed thickness (*RBTHICK*), and riverbed

Table 4. River Boundary Parameters (The Thai Royal Irrigation Department, 2015)

River Name	*RSTAGE* (m)		*RBBOT* (m)		*COND* (m^2/day)	
	Minimum	Maximum	Minimum	Maximum	Minimum	Maximum
Chao Phraya	-5.63	19.85	-12.39	-0.45	232	15,302
Mae Klong	-6.37	3.72	-6.62	0.31	526	6,688
Pa Sak	-4.59	17.66	-12.69	7.60	1,588	8,709
Tha Chin	-3.03	3.46	-4.32	-2.82	174	2,458

Note: Heights in m are referred to MSL.

hydraulic conductivity (K_z) data were determined from the Thai Royal Irrigation Department data (2015). The riverbed K_z values were estimated, using permeability lab test. Table 4 tabulates the river stage (*RSTAGE*), riverbed bottom (*RBBOT*) and riverbed conductance (*COND*) of the four rivers.

3.7 Pumping

The LCP basin has 8,330 legal groundwater pumping wells, with a total pumping rate set by law in each province, leading to a total of ~0.65 million m^3/day. For each well data consist of the location, screening depth and permitted pumping rate. These permitted groundwater pumping rates were used to represent pumping in this study. The groundwater pumping rates based on permitted pumping rates in PD and NL was ~0.25 million m^3/day and in NB ~0.1 million m^3/day.

For this reason, this research focused on the three aquifers – the PD, NL, and NB aquifers – due to their heavy use for consumption, industry, and agriculture and the availability of data. Although the BK aquifer is close to the ground surface, water has not been drawn, due to seawater intrusion and chloride levels beyond the drinking water standard (The Thai Ministry of Natural Resources and Environment, 2009). The model also includes the SK, PT, TB and PN aquifers, but these have not been pumped significantly, because the aquifers are deep, making groundwater extraction expensive.

Figure 7 shows the groundwater extraction rate in each province. Low pumping wells in Bangkok and vicinity were a consequence of DGR groundwater control, whereas, high pumping is due to industry. High total pumping rates in paddy and crop fields, from many widely distributed wells, did not cause the hydraulic head to drop significantly, whereas industrial pumping did cause the head to drop.

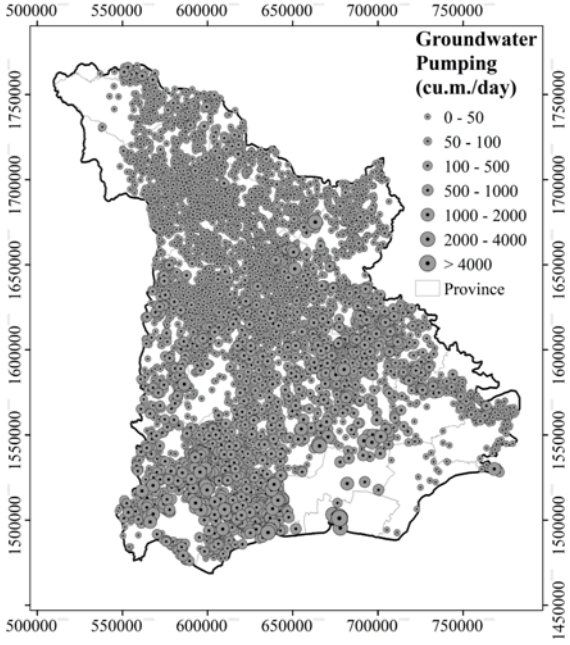

Fig. 7. Groundwater Pumping Rate in the LCP Basin

3.8 Simulation Strategy

Because a primary purpose of this paper was to explore the interplay between *dh*/*dz* and vertical anisotropy, we first simulated the effects of K_h/K_v on the regional performance of the model. Next, we explored the effects of recharge and pumping on the simulated values of *dh*/*dz* by varying recharge and pumping within plausible ranges. Although, additional calibration of the model could improve agreement between measured and modeled heads, here we concentrated on the vertical anisotropy and the ability to calibrate it in a model of this type. Future studies will likely be able to further improve the model through calibration of spatial variations in K_h and other variables.

3.8.1 Vertical Hydraulic Gradient Simulation vs Measured Values

We first attempted to assess the accuracy of the groundwater model. We stepped through K_h/K_v values from 10^1 to 10^5, by adjusting K_v to ascertain the anisotropy resulting in the best agreement between measured and simulated regional vertical hydraulic gradients. Because we had excellent data on vertical gradients and they are very sensitive to vertical anisotropy (Fogg, 1986), we generated the model by adjusting K_v to achieve good representation of the vertical gradients, i.e., correlation coefficient (R^2) ≥ 0.8. Because smaller vertical gradients can indicate lower K_v, or greater vertical connectivity in the aquifers, we also explored the interplay between connectivity and gradients.

3.8.2 Sensitivity to Pumping and Recharge

Previous groundwater models are sensitive to change in pumping and recharge rate, because these vary the hydraulic head and quantity of groundwater in the system (Pholkern et al., 2018; Taweesin et al., 2018). We investigated sensitivity by changing the parameters in the model, one by one and recalculating, to determine the vertical gradient (relative to experimental values) caused by changes in each parameter. Pumping and recharge rates were varied by ± 10% and ± 20%, one at a time. For this experiment, the anisotropy was fixed to 10^3 – 10^4, based on results from the previous experiment (section 3.8.1.) which showed good agreement for values in those ranges.

3.8.3 Matching Measured vs Simulated Hydraulic Head

We attempted to accurate the groundwater model by matching measured and simulated hydraulic head because the optimal model has to agreement both of *h* and *dh*/*dz* match. We evaluated sensitivity by using PEST (Doherty and Hunt, 2010), with manual calibration, by changing *K* parameters in the model. The model was considered acceptable, when the groundwater fitting error was reasonable, i.e., standard error (SE) ≤ 0.5 m, root mean square error (RMSE) and normalized root mean square error (NRMSE) ≤ 10% and R^2 ≥ 0.9 (Du et al., 2018).

4. Results and Discussion

This section focuses on the computed vertical gradients compared

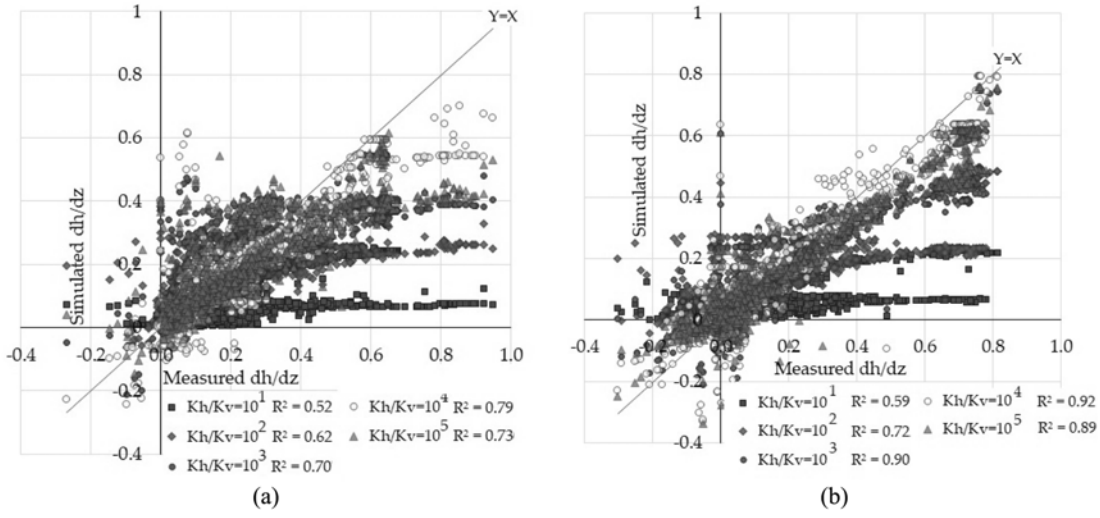

Fig. 8. Measured vs Simulated Vertical Hydraulic Gradients for Anisotropies of 10^1 – 10^5: (a) PD-NL, (b) NL-NB (A high frequency of points along the Y = X line represents good agreement between measured and simulated values.)

to the measurements (i.e., Fig. 4). We also checked whether the model indicated a lower limit for K_v.

4.1 Simulated Vertical Hydraulic Gradient

The correlation between the simulated and measured dh/dz with K_h/K_v values of 10^1 – 10^5 was tested. The simulated dh/dz was computed by gridding the hydraulic head change in each aquifer and divided by the distance between the middle of aquifers. Low correlations indicated low anisotropy accuracy, whereas high correlation along the Y=X line in Fig. 8, for each tested K_h/K_v, indicated a good fit for that ratio.

For $K_h/K_v = 10^1$, the simulated $dh/dz \rightarrow 0$, because the anisotropy was too low, meaning that the vertical hydraulic conductivity was too high. In other words, hydraulic head in the adjacent layers essentially equilibrated in the model, clearly indicating $K_h/K_v = 10^1$ was impractical, although the simulated h was a reasonable match with the measured one.

As anisotropy increased from 10^1 to 10^3 and 10^4, the model was better able to reproduce the measured dh/dz values. The best R^2 occurred at $K_h/K_v = 10^4$; but, because many of the simulated values of dh/dz were higher than the measured values, the results suggest that $K_h/K_v = 10^4$ was an upper limit to the anisotropy. This, together with the fact that the simulated dh/dz values, for $K_h/K_v = 10^3$, were lower than the measured values, would suggest that the actual regional value of anisotropy was between 10^3 and 10^4. $K_h/K_v = 10^5$ resulted in a lower correlation than the 10^4 case, suggesting that an anisotropy of 10^5 was implausibly high.

There were more scatters for the PD-NL aquifers than those in NL-NB aquifer. This can be seen from Fig. 8. K_v values had greater variability between these two aquifers and led to a complex pattern of K_h/K_v values for the PD-NL aquifers as R^2 was lower.

Because dh/dz was also influenced by recharge and pumping, one should examine estimates of K_h/K_v, assuming estimated amounts and distributions of recharge and pumping. In the next section, the roles of pumping and recharge were explored.

4.2 Sensitivity Analysis - Recharge and Pumping

It is well known that the distribution of hydraulic head can be altered by the influence of recharge and pumping (Pholkern et al., 2018; Taweesin et al., 2018). Accordingly, errors in the recharge or pumping could lead to erroneous calibrated estimates of K_v. So, this section explores sensitivity between dh/dz, recharge and pumping. The strong vertical gradients were made possible by strong vertical anisotropy, but dh/dz was also driven by recharge and pumping.

Figures 9 and 10 show the sensitivity of simulated dh/dz to recharge and pumping rates. The simulated dh/dz was computed as described above. The low correlation indicated high sensitivity of the groundwater model to the parameters. The increasing recharge led to more upper aquifer inflow, groundwater flow increased from upper to lower aquifers, and led to a higher dh/dz. The decreased recharge contributed to less inflow; groundwater flow rate from upper to lower aquifer was reduced, so that dh/dz declined. Increased pumping contributed to aquifer drawdown, extended the cone of depression, which changed the hydraulic head and led to change in dh/dz. The groundwater flow increased the velocity near the pumping wells, because of higher groundwater flow, from upper to lower aquifers. The decreased pumping reduced the aquifers drawdown, which, in turn, reduced the cone of depression, so that the dh/dz outside the cone of depression was still constant. Then, for some locations, the correlations did not change.

Figures 9 show the correlation between measured and simulated dh/dz for recharge rates for K_h/K_v of 10^3 and 10^4. In the PD-NL aquifer, the measured *vs* simulated correlation for dh/dz showed that both anisotropies were sensitive to recharge, because recharge strongly affected the hydraulic head, which, in turn, significantly affected dh/dz. While, in the NL-NB aquifer, dh/dz, at anisotropy

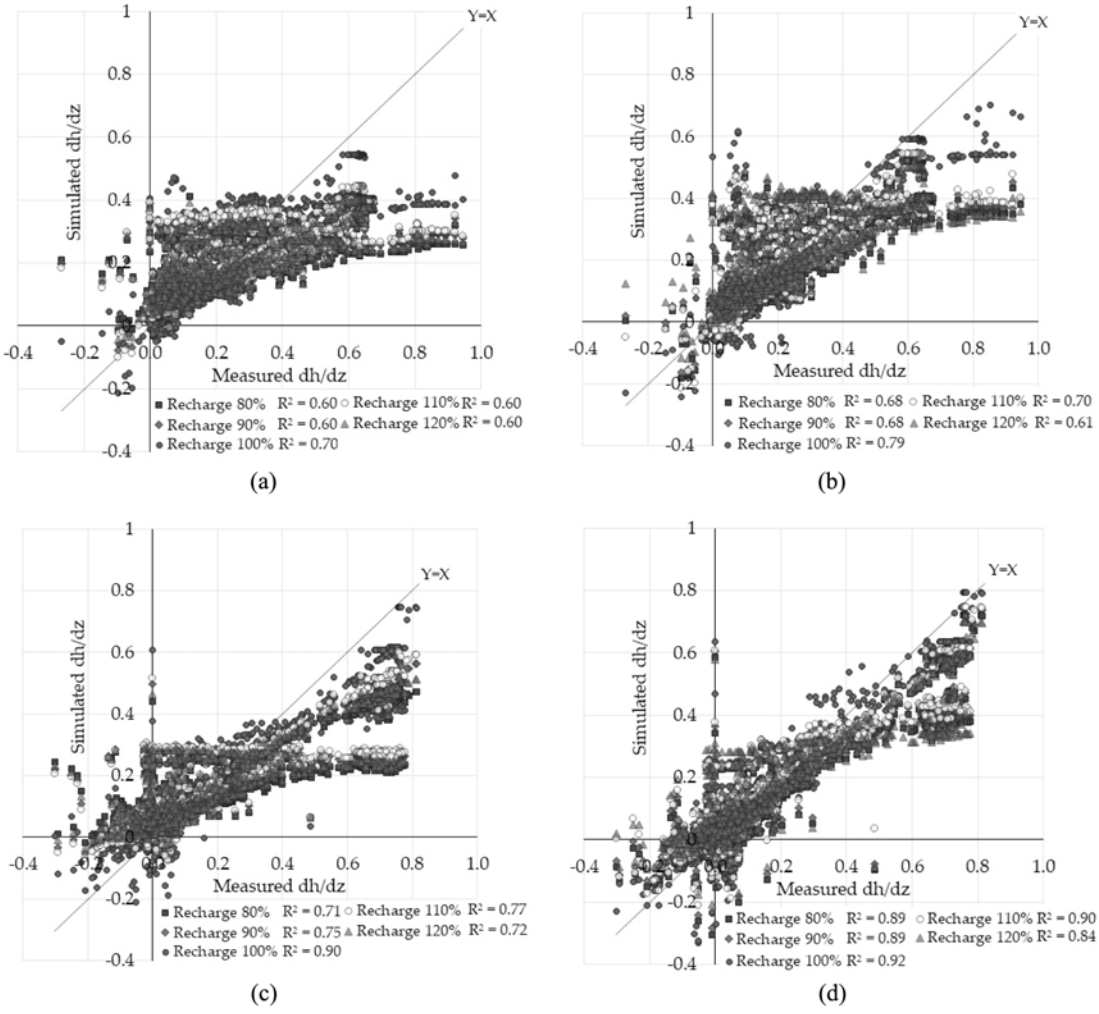

Fig. 9. Sensitivity Analysis of Recharge: (a) Anisotropy of 10^3 for PD-NL, (b) Anisotropy of 10^3 for NL-NB, (c) Anisotropy of 10^4 for PD-NL, (d) Anisotropy of 10^4 for NL-NB

of 10^4, was less sensitive to recharge, because the high anisotropy in the upper layer obstructed groundwater recharge to the lower aquifer, so *dh*/*dz* was not sensitive to recharge. Interestingly, both PD-NL aquifers *dh*/*dz* values were more sensitive than the NL-NB *dh*/*dz* ones, because the recharge rapidly added to the aquifer and became groundwater, indicating that *dh*/*dz* in the shallower aquifer was strongly affected by recharge.

Figures 10 show the correlation between the measured and simulated *dh*/*dz* for pumping rates for K_h/K_v of 10^3 and 10^4. The measured *vs* simulated correlation for *dh*/*dz* in both anisotropies were sensitive to pumping in the PD-NL aquifer, because pumping contributed to the drawdown, which led to fluctuations in *dh*/*dz*. Meanwhile, *dh*/*dz* for anisotropy of 10^4 was less sensitive to pumping in the NL-NB aquifer, due to the high anisotropy and low pumping rate in the NB aquifer. Change in pumping was not enough to increase drawdown with an anisotropy of 10^4, so *dh*/*dz* was less changed, and groundwater then moved horizontally. Interestingly, *dh*/*dz* values in the PD-NL aquifer were more sensitive than in the NL-NB aquifer, because the relatively high pumping rate contributed to higher drawdown, that, in turn, contributed to greater differences in *h* and *dh*/*dz*.

The correlations between measured and simulated *dh*/*dz* of recharge and pumping were lower than the normal ones, because the hydraulic equilibrium was perturbed and the groundwater should approach equilibrium. Then, *dh*/*dz* values were changed as groundwater flowed across the aquifers. Comparing Figs. 9 and 10, we see that recharge was more sensitive than pumping, in the simulated *dh*/*dz*, because the correlation was lower under recharge, than with pumping.

4.3 Measured vs Simulated Hydraulic Head

Although, the measured and simulated *dh*/*dz* values were comparable, the *h* must be comparable also. This section checked *h* for anisotropies of 10^1, 10^3 and 10^4, see Fig. 11 and Table 5. The result showed that $K_h/K_v = 10^3$ provided a better correlation with *h*, thus the anisotropy that provide better simulated *h* did not guarantee the best *dh*/*dz*. because $K_h/K_v = 10^4$ showed the best correlation of *dh*/*dz*. The cause of better hydraulic head matching

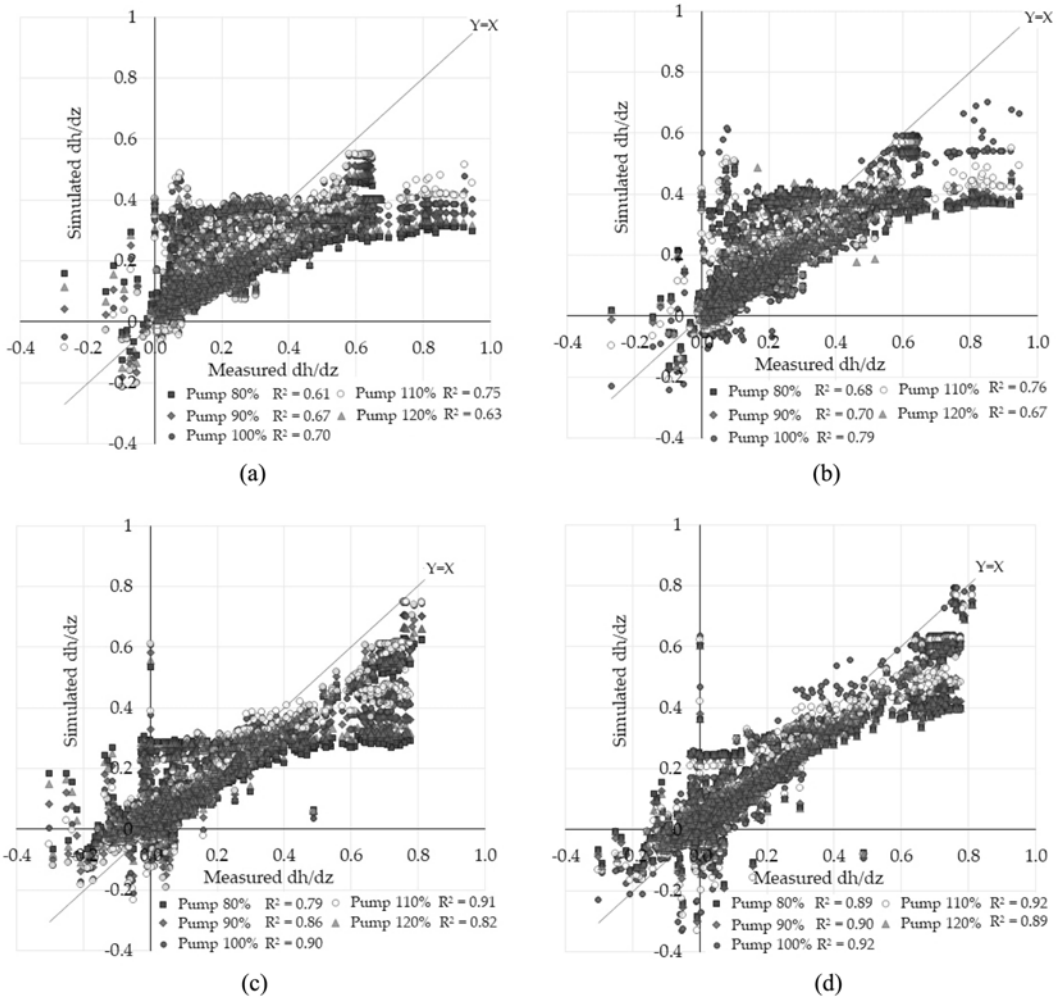

Fig. 10. Sensitivity Analysis of Pumping: (a) Anisotropy of 10^3 for PD-NL, (b) Anisotropy of 10^3 for NL-NB, (c) Anisotropy of 10^4 for PD-NL, (d) Anisotropy of 10^4 for NL-NB

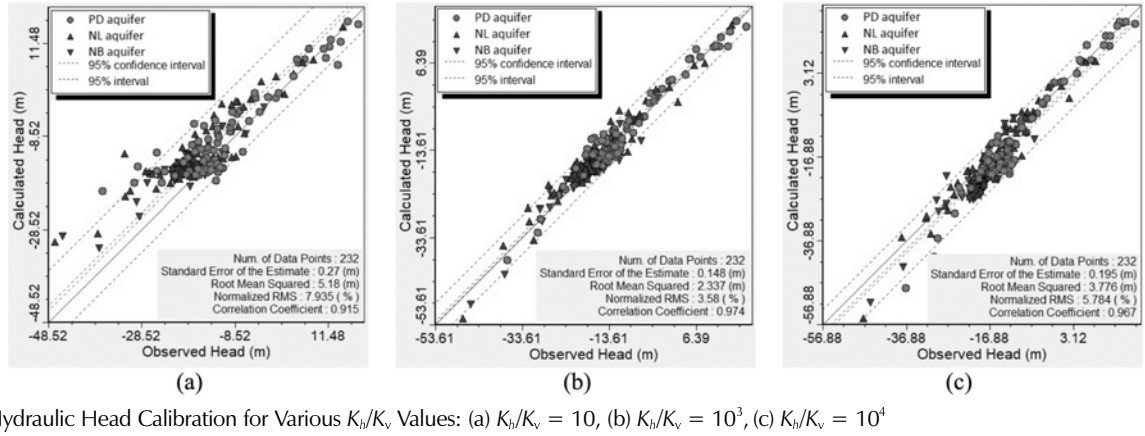

Fig. 11. Hydraulic Head Calibration for Various K_h/K_v Values: (a) $K_h/K_v = 10$, (b) $K_h/K_v = 10^3$, (c) $K_h/K_v = 10^4$

Table 5. Model Results

K_h/K_v	SE (m)	RMSE (%)	NRMSE (%)	Mean R^2 for h	Mean R^2 for dh/dz
10^1	0.27	5.18	7.93	0.91	0.55
10^3	0.14	2.33	3.58	0.97	0.80
10^4	0.19	3.77	5.78	0.96	0.85

Note: SE = standard error, RMSE = root mean squared error, NRMSE = normalized root mean squared error, R^2 = correlation coefficient

for K_h/K_v = 10^3 was that the observation wells were in the discontinuous zone, with low anisotropy. If we did not draw the *dh*/*dz* maps (Fig. 4), hydraulic head matching would mislead the anisotropy. This shows that the *h* and *dh*/*dz* accuracy are important to improve groundwater models, especially, regional sediment models with high K_h/K_v.

5. Conclusions

Using a large database of 3D hydraulic head (*h*) data, we explored the interplay between vertical anisotropy (K_h/K_v) and vertical hydraulic gradients (*dh*/*dz*) in a classic sedimentary groundwater basin containing multiple aquifers and abundant aquitard strata. We demonstrated the value of 3D *h* data for model calibration, while also showing the strong sensitivity between K_h/K_v and *dh*/*dz*, where, until K_h/K_v increased to values in the 10^3 – 10^4 range, the model was unable to even approximate the measured values of *dh*/*dz*. This also confirms, as suggested by Fogg (1986), that the initial calibration step in such a system should be tuning of K_h/K_v to find the threshold at which simulated and measured values of *dh*/*dz* agree. In contrast, many previous calibration efforts simply assumed K_h/K_v values and concentrated on calibrating horizontal hydraulic conductivity (K_h) or horizontal transmissivity (T_h) (Saraphirom et al., 2013; Pholkern et al., 2018; Taweesin et al., 2018).

We also showed that the calibrated values of K_h/K_v were sensitive to errors in recharge and pumping. Recharge led to change in inflow groundwater, that led to head change, which, in turn, led to change in *dh*/*dz*. While, pumping contributed to aquifer outflow, change in head drawdown, around the radius of influence, changed *dh*/*dz*. Additionally, in a shallower aquifer, *dh*/*dz* was more strongly affected by recharge and pumping, because high K_h/K_v, in an upper aquifer, obstructed groundwater flow to the lower aquifer.

Our mapping of *dh*/*dz* revealed localities with low vertical gradients, indicating potentially good vertical connectivity, or relatively high vertical hydraulic conductivity (K_v). Future work should exploit the large data base of *h* and *dh*/*dz* values to better estimate regional and local K_h/K_v variations. This will help identify local zones of good vertical connectivity, that are of special significance for managing groundwater quantity and quality. For example, such zones could represent important recharge zones for deep confined aquifers, while also representing contamination threats, if the shallow aquifers become contaminated.

Acknowledgements

We thank the Thailand Research Fund through the Royal Golden Jubilee Ph.D. Program, Grant No. PHD/0189/2556 for the financial sponsorship. Thanks to the Thai Land Development Department, Thai Meteorological Department, Thai Royal Irrigation Department and Thai Department of Groundwater Resources for data. Special thanks also go to Dr. Christopher T. Green (U.S. Geological Survey) and Prof. Timothy R. Ginn (Washington State University) for their comments and suggestions.

ORCID

Pinit Tanachaichoksirikun https://orcid.org/0000-0001-8168-1837

References

AIT (1981) Investigations of land subsidence caused by deep well pumping in the Bangkok area. Comprehensive Report 1978-1981, Asian Institute of Technology, Bangkok, Thailand

Arlai P, Koch M (2006) Statistical and stochastic approaches to assess reasonable calibrated parameters in a complex multi-aquifer system. Proceedings of CMWR XVI – Computational methods in water resources, June 19, Copenhagen, Denmark, DOI: 10.4122/1.1000000338

Bear J (1972) Dynamics of fluids in porous media. Elsevier, New York, NY, USA

Belitz K, Phillips SP, Gronberg JM (1993) Numerical simulation of ground-water flow in the central part of the Western San Joaquin valley, California. United States Geological Survey Water-Supply Paper 2396, United States Geological Survey, Reston, VA, USA, DOI: 10.3133/wsp2396

Cox JB (1968) A review of engineering properties of the recent marine clays in Southeast Asia. Research Report No. 6, Asian Institute of Technology, Pathum Thani, Thailand

Dawoud MA, Allam AR (2004) Effect of new nag hammadi barrage on groundwater and drainage conditions and suggestion of mitigation measures. *Water Resources Management* 18(4):321-337, DOI: 10.1023/B:WARM.0000048484.39933.9e

DGR (2010) Creating a geographic information system for groundwater management in the groundwater crisis zone. Thai Department of Groundwater Resources, Bangkok, Thailand

DGR (2012) Effect of underground structure due to the restoration of water pressure in Bangkok and vicinity. Thai Department of Groundwater Resources, Bangkok, Thailand

DGR (2015) Groundwater situation in Thailand 2015 quarter 1. Thai Department of Groundwater Resources, Bangkok, Thailand

Doherty J, Hunt R (2010) Approaches to highly parameterized inversion: A guide to using PEST for groundwater-model calibration. Scientific Investigations Report 2010-5169, United States Geological Survey, Reston, VA, USA

Du X, Lu X, Hou J, Ye X (2018) Improving the reliability of numerical groundwater modeling in a data-sparse region. *Water* 10(3):1-15, DOI: 10.3390/w10030289

Fogg GE (1986) Groundwater flow and sand body interconnectedness in a thick, multiple-aquifer system. *Water Resources Research* 22(5): 679-694, DOI: 10.1029/WR022i005p00679

Fogg GE, Carle SF, Green C (2000) Connected-network paradigm for the alluvial aquifer system. *Geological Society of America* 348:25-42, DOI: 10.1130/0-8137-2348-5.25

Fogg GE, Noyes CD, Carle SF (1998) Geologically based model of heterogeneous hydraulic conductivity in an alluvial setting. *Hydrogeology Journal* 6(1):131-143, DOI: 10.1007/s100400050139

Fornés J, Pirarai K (2014) Groundwater in Thailand. *Journal of Environmental Science and Engineering* 3:304-315, DOI: 10.17265/2162-5263/2014.06.003

Galloway DL, Burbey TJ (2011) Review: Regional land subsidence accompanying groundwater extraction. *Hydrogeology Journal* 19(8): 1459-1486, DOI: 10.1007/s10040-011-0775-5

Gupta AD, Babel MS (2005) Challenges for sustainable management of

groundwater use in Bangkok, Thailand. *International Journal of Water Resources Development* 21(3):453-464, DOI: 10.1080/07900620500036570

Harbaugh AW, Banta ER, Hill MC, Mcdonald MG (2000) MODFLOW-2000, the U.S. geological survey modular ground-water model-user guide to modularization concepts and the ground-water flow process. Open-File Report 2000-92, United States Geological Survey, Reston, VA, USA, DOI: 10.3133/ofr200092

Heilweil VM, Hsieh PA (2006) Determining anisotropic transmissivity using a simplified Papadopulos method. *Ground Water* 44(5):749-753, DOI: 10.1111/j.1745-6584.2006.00210.x

Hoque MA, Burgess WG (2012) 14C dating of deep groundwater in the Bengal aquifer system, Bangladesh: Implications for aquifer anisotropy, recharge sources and sustainability. *Journal of Hydrology* 444-445: 209-220, DOI: 10.1016/j.jhydrol.2012.04.022

Izady A, Abdalla O, Joodavi A, Chen M (2017) Groundwater modeling and sustainability of a transboundary hardrock-alluvium aquifer in North Oman mountains. *Water* 9(3):1-17, DOI: 10.3390/w9030161

JICA (1995) The study on management of groundwater and land subsidence in the Bangkok metropolitan area and its vicinity, JICA Report No. 11194610, Japan International Cooperation Agency, Tokyo, Japan

Jiménez-Madrid A, Castaño S, Vadillo I, Martinez C, Carrasco F, Soler A (2017) Applications of hydro-chemical and isotopic tools to improve definitions of groundwater catchment zones in a karstic aquifer: A case study. *Water* 9(8):1-21, DOI: 10.3390/w9080595

Kasetsart University (2004) Effects of groundwater recharge on land subsidence and groundwater quality: Mathematical model study. Final Project Report, Department of Groundwater Resources, Bangkok, Thailand

LDD (2015) Soil resource. Thai Land Development Department, Retrieved September 10, 2015, http://www.ldd.go.th/ldd_en/

Michael HA, Voss CI (2009) Estimation of regional-scale groundwater flow properties in the Bengal basin of India and Bangladesh. *Hydrogeology Journal* 17(6):1329-1346, DOI: 10.1007/s10040-009-0443-1

Patriarche D, Castro MC, Goblet P (2004) Large-scale hydraulic conductivities inferred from three-dimensional groundwater flow and ^{4}He transport modeling in the Carrizo aquifer, Texas. *Journal of Geophysical Research: Solid Earth* 109(11):1-19, DOI: 10.1029/2004JB003173

Phien-wej N, Giao PH, Nutalaya P (2006) Land subsidence in Bangkok, Thailand. *Engineering Geology* 82(4):187-201, DOI: 10.1016/j.enggeo.2005.10.004

Pholkern K, Saraphirom P, Srisuk K (2018) Potential impact of climate change on groundwater resources in the Central Huai Luang basin, Northeast Thailand. *Science of the Total Environment* 633:1518-1535, DOI: 10.1016/j.scitotenv.2018.03.300

Piancharoen C (1977) Groundwater and land subsidence in Bangkok, Thailand. *IAHS Publication* 121:355-364

Piancharoen C, Chuamthaisong C (1978) Groundwater of bangkok metropolis, Thailand. *IAH Memoire* 11:510-528

Ramnarong V (1999) Evaluation of groundwater management in Bangkok: Positive and negative. In: Groundwater in the urban environment: Selected city profiles. Balkema Publishers, Rotterdam, Netherlands, 51-62

Samper-Calvete FJ, García-Vera MA (1998) Inverse modeling of groundwater flow in the semiarid evaporitic closed basin of Los Monegros, Spain. *Hydrogeology Journal* 6(1):33-49, DOI: 10.1007/s100400050132

Sanford W (2011) Calibration of models using groundwater age. *Hydrogeology Journal* 19(1):13-16, DOI: 10.1007/s10040-010-0637-6

Saraphirom P, Wirojanagud W, Srisuk K (2013) Potential impact of climate change on area affected by waterlogging and saline groundwater and ecohydrology management in Northeast Thailand. *Environment Asia* 6(1):19-28

Seeboonruang U (2014) An empirical decomposition of deep groundwater time series and possible link to climate variability. *Global NEST Journal* 16(1):87-103

Seeboonruang U (2018) Wavelet relationship between climate variability and deep groundwater fluctuation in Thailand's central plains. *KSCE Journal of Civil Engineering* 22(2):868-876, DOI: 10.1007/s12205-017-1597-3

Sheets RA, Bair ES, Rowe GL (1998) Use of ^{3}H/^{3}He ages to evaluate and improve groundwater flow models in a complex buried-valley aquifer. *Water Resources Research* 34(5):1077-1089, DOI: 10.1029/98WR00007

Štuopis A, Juodkazis V, Mokrik R (2012) The quaternary aquifer system flow model by chemical and tritium isotope data: Case of south-east Lithuania. *Baltica* 25(2):91-98, DOI: 10.5200/baltica.2012.25.09

Sun H, Grandstaff D, Shagam R (1999) Land subsidence due to groundwater withdrawal: Potential damage of subsidence and sea level rise in Southern New Jersey, USA. *Environmental Geology* 37(4):290-296, DOI: 10.1007/s002540050386

Tanachaichoksirikun P, Seeboonruang U, Saraphirom P (2018) Impact of climate change on the groundwater sustainability in the Lower Chao Phraya Basin, Thailand. Proceedings of 4th international conference on engineering, appllied sciences and technology, July 4-7, Phuket, Thailand

Taweesin K, Seeboonruang U, Saraphirom P (2018) The influence of climate variability effects on groundwater time series in the lower central plains of Thailand. *Water* 10(3):1-23, DOI: 10.3390/w10030290

Thai Department of Mineral Resource (2001) Geology of Thailand: Commemoration of the 72nd anniversary of his majesty king Bhumibol Adulyadej's birthday December 5, 1999. Department of Mineral Resource, Bangkok, Thailand

Thai Ministry of Natural Resources and Environment (2009) Criteria and measure definition of the public health and poison protection. Ministry of Natural Resources and Environment, Retrieved August 11, 2019, http://www.pcd.go.th/info_serv/reg_std_water01.html

Thai Royal Irrigation Department (2015) Central region irrigation hydrology center. Royal Irrigation Department Thailand, Retrieved October 9, 2015, http://hydro-5.rid.go.th/

TMD (2015) Thai weather. Meteorological Department, Retrieved September 10, 2015, https://www.tmd.go.th/index.php

Todd DK, Mays LW (1980) Groundwater hydrology, 3rd edition. John Wiley & Sons, Inc., Hoboken, NJ, USA, 1-636

Winter TC, Pfannkuch HO (1984) Effect of anisotropy and groundwater system geometry on seepage through lakebeds, 2. Numerical simulation analysis. *Journal of Hydrology* 75(1-4):239-253, DOI: 10.1016/0022-1694(84)90052-0

Zlotnik VA, Cardenas MB, Toundykov D (2011) Effects of multiscale anisotropy on basin and hyporheic groundwater flow. *Ground Water* 49(4):576-583, DOI: 10.1111/j.1745-6584.2010.00775.x